Tool wear mechanisms and effects on refill friction stir spot welding of AA2198-T8 sheets

Castro, Camila C. de; Shen, Junjun; Plaine, Athos H.; Suhuddin, Uceu F.H.; Alcântara, Nelson Guedes de; Santos, Jorge F. dos; Klusemann, Benjamin

Published in:
Journal of Materials Research and Technology

DOI:
10.1016/j.jmrt.2022.07.092

Publication date:
2022

Document Version
Publisher's PDF, also known as Version of record

JOURNAL OF MATERIALS RESEARCH AND TECHNOLOGY 2022;20:857–866

Available online at www.sciencedirect.com

jmr&t Journal of Materials Research and Technology

journal homepage: www.elsevier.com/locate/jmrt

Original Article

Tool wear mechanisms and effects on refill friction stir spot welding of AA2198-T8 sheets

Camila C. de Castro [a,*], *Junjun Shen* [a], *Athos H. Plaine* [b], *Uceu F.H. Suhuddin* [a], *Nelson Guedes de Alcântara* [c], *Jorge F. dos Santos* [a], *Benjamin Klusemann* [a,d]

[a] *Helmholtz-Zentrum Hereon, Institute of Materials Mechanics, Solid State Materials Processing, Geesthacht, Germany*

[b] *Santa Catarina State University, Department of Mechanical Engineering, Joinville, Santa Catarina, Brazil*

[c] *Federal University of Sao Carlos, Department of Materials Engineering, São Carlos, São Paulo, Brazil*

[d] *Leuphana University Lüneburg, Institute of Product and Process Innovation, Lüneburg, Germany*

ARTICLE INFO

Article history:
Received 15 June 2022
Accepted 14 July 2022
Available online 19 July 2022

Keywords:
Tool wear
Friction-based joining processes
Refill friction stir spot welding
Refill FSSW
AA2198

ABSTRACT

Refill Friction Stir Spot Welding (refill FSSW) is a method for joining similar and dissimilar lightweight metallic materials or thermoplastic polymers. The technique produces welds that feature suitable mechanical properties with advantages such as the possibility of industrial scalability and automation. Still, some challenges need to be overcome in order to increase the adoption of this technique in industry. Tool wear is a key issue for friction-based processes, since it impacts the process costs and quality of the welds. In this study, a total of 2350 welds of AA2198-T8 sheets were performed and the effect of wear on probe and shoulder was investigated. While the probe did not suffer any considerable wear after this number of welds, the shoulder underwent wear in different areas, with distinct wear mechanisms. Adhesive wear and plastic deformation were determined as the primary damage mechanisms affecting different areas of the shoulder. Mechanical testing of selected welds has shown a trend towards reduction in the lap shear strength (*LSS*) as a function of tool wear. Macrostructural analysis of welds' geometrical features shows that profile changes at the shoulder due to wear led to a trend of reduction in stirred zone area and, consequently, joints' *LSS*. Modifications in the worn shoulder profile were suggested as possible causes for changes in hook height, which was identified as a further determining factor to the observed reduction in *LSS*. Still, all tested welds surpassed the minimum lap shear strength standard requirements for aeronautical applications.

* Corresponding author.
E-mail address: camila.castro@hereon.de (C.C. de Castro).

https://doi.org/10.1016/j.jmrt.2022.07.092

1. Introduction

Tool wear is a key issue concerning solid-state joining processes. It impacts not only the quality of produced welds – mechanical properties and its variability along with the welding cycles – but also affects dimensional features of the tool, reducing the tool life cycle and thus, increasing production costs and reducing productivity [1–3]. The friction between two unlubricated interfaces is controlled by adhesion (when particles of both surfaces bond), ploughing (caused by asperities on the harder material surface) and/or deformation – complex mechanisms which all combined result in wear [4].

The interaction between two material interfaces with a significant difference in hardness at direct physical contact is defined as abrasive wear. This mechanism likely plays a significant role for Friction Stir Welding (FSW) tools used in joining of aluminum metal-matrix composites (MMC). Prado et al. [5] studied the influence of ceramic particles in the base material on the wear of O-1 AISI tool-steel screw probe by comparing the welding of AA6061-T6 plates with two different compositions: (i) standard AA6061-T6 and (ii) AA6061-T6 with 20 vol.% Al_2O_3 particles, using the same rotational speed of 1000 rpm. It was demonstrated that no measurable wear was found after the joining of the AA6061-T6 plates, while the tool suffered an effective wear rate of 0.64%/cm in welding of the MMC plates. In addition to the influence of ceramic particles, other studies also associate the tool wear to the process parameters, and reported that the tool wear increases for higher weld speed for AA6061-T6 + 20 vol.% Al_2O_3 [6], and AA2124-T4 + 25% SiC [3]. For FSW of cast-aluminum 359 + SiC MMCs [7], higher wear was found for high rotational speed and low weld speed.

In the case of friction-based welding of unreinforced metallic alloys, other wear mechanisms are predominant on tool degradation, considering that the tool material exhibits higher hardness than the sheet material. Choi et al. [8] concluded that the damage underwent by WC-Co tools during Friction Stir Spot Welding (FSSW) of steel sheets may be a result of oxidative wear of the WC surface, formation of a W–Fe–O ternary compound and fatigue. Wang et al. [9] studied FSW of Ti–6Al–4V alloy and associated the damage suffered by the WC-Co tool to the chemical affinity between C and Ti at high-temperature conditions. The affinity between these two materials leads to adherence of the sheet material on the tool, which may result in detaching of particles of this adhered material layer under mechanical interaction between the parts during the process. Nasiri et al. [10] investigated microstructural changes of a severely damaged tool caused by refill friction stir spot welding (refill FSSW) of AA2099 and associated the rapid degradation of the shoulder with the formation of brittle intermetallics on the tool's surface due to heating combined with high Li content of the base material.

Refill FSSW is a friction-based welding technique developed at Helmholtz-Zentrum Hereon [11] to join similar or dissimilar lightweight materials such as aluminum [12], magnesium [13], titanium [14] as well as hybrid metal-polymer joints [15]. The sheets are welded in a lap configuration resulting in a joint free of the characteristic residual keyhole associated with the FSSW process [16]. Refill FSSW has received considerable attention for aeronautical applications [17] as an option to replace mechanical fastening for joining aluminum parts in aircraft designs, resulting in weight-saving of structures and consequent reduction of fuel consumption.

The three-piece tool used in refill FSSW consists of clamping ring, shoulder and probe, as presented in Fig. 1. The clamping ring is the stationary part of the tool and plays the role of keeping the sheets together during the process, while the probe and shoulder are the rotating parts that can be moved along the plunging direction. The process starts with the displacement of the tool set in the direction of the sheets. As soon as the tool reaches the workpiece surface, the clamping mechanism is activated (Fig. 2(a)). The rotating shoulder is then plunged into the material causing its plasticization, as a result of the heat input and shear stresses. As the shoulder plunges progressively deeper into the worksheet, the plasticized material flows into the cavity generated by the retraction of the probe (Fig. 2(b)). Afterwards the probe and shoulder move towards the workpiece surface, pushing the plasticized material back (Fig. 2(c)). Finally, the clamping force is release and the set of tools lifted, leaving the spot weld (Fig. 2(d)).

Investigations on tool wear mechanisms in refill FSSW are scarcely available in the literature. For instance, Montag et al. [18] evaluated the effects of wear in refill FSSW of AA6082-T6 sheets. Different locations of the shoulder surface were observed, and the study shows that the region most intensively in contact with the clamping ring is the most damaged zone of the tool. No correlation between welds' lap shear strength (*LSS*) and tool wear was identified. Lauterbach et al. [19] compared the effect of three different wear-resistant coatings (CrVN, WC and TiBN–TiB_2) and local hardening (nitriding) on refill FSSW tools. The application of the coating led to a decrease in the wear rate until the coating layer was worn out, exposing the tool material. This enables the formation of intermetallic compounds and dramatically increases the wear process on the tool. De Carvalho et al. [20] studied the variation of joints' *LSS* through 2500 welding cycles using a H13 shoulder and 6061-T6 sheets and associated the reduction on welds' mechanical resistance to the change in the fracture mode after 2000 produced welds. The findings also indicate that the tool

Fig. 1 – Refill FSSW 3-piece tool: probe, shoulder and clamping ring and tool assembly.

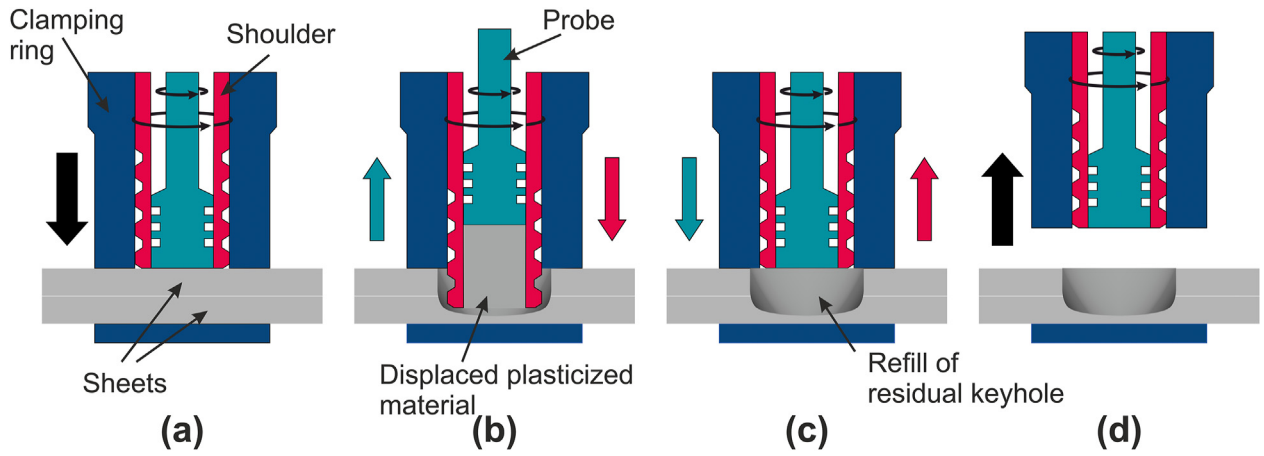

Fig. 2 – Schematic representation of the shoulder-plunge refill FSSW mode: (a) clamping of the sheets, (b) shoulder plunging and probe retraction, (c) shoulder and probe reaching back the sheet's surface and refilling the keyhole and (d) releasing of the clamping force and tool set lifting.

wear reduces the energy input during refill FSSW, impacting the hardness of the produced joint.

The present work aims to discuss the wear mechanisms controlling the dimensional changes on the refill FSSW probe and shoulder throughout the welding of 2350 spots on AA2198 1.6 mm–thick sheets. Furthermore, the *LSS* behavior is investigated, based on tests conducted on selected spot welds out of the 2350 joints and their variability. A correlation of *LSS* with cross-sectional macrostructural features is also herein addressed.

2. Materials and methods

2.1. Tool material and characterization

All tool parts used in this study (probe, shoulder and clamping ring) consisted of molybdenum-vanadium-alloyed Hotvar® tool steel, whose chemical composition, heat treatment specifications and overall mechanical properties are presented in Table 1. To investigate the wear suffered by the tool, probe and shoulder, Fig. 3, were measured by a Mahr Multiscope 250 profilometer at different stages of the study: an as-received tool, s_0, used as reference for the experiment and after several performed welds, s_{1350} and s_{2350} after 1350 and 2350 number of spot welds, respectively. The measurement of the tool at these specific number of spots were chosen according to a reduction of around 10% in *LSS*, and 1000 welding cycles after this point, respectively. These numbers were conveniently chosen due to the expected and observed changes in the weld properties. To remove all aluminum adhered to the surface, all three tool parts were cleaned by a 3 h immersion in NaOH solution before each measurement.

2.2. Welding of specimens

A total of 2350 sequential refill FSSW joints were produced on AA2198-T8 (nominal chemical composition (wt. %) of 3.4% Cu, 0.8% Li, 0.27% Mg, 0.18% Ag, 0.10% Zr and Al balance) overlapped sheets (1.6 mm thick). The 2350 welds were divided into different sets, limited by each disassembly of the tool, cleaning, characterization and reassembly: set A corresponds to the initial 1350 welds; set B, between 1350 and 2000 welds, and set C to the final 350 welds. Specimens for *LSS* tests were prepared by welding two 126 × 35 × 1.6 mm^3 (length x width x thickness) sheets overlapped by 46 mm, according to ISO 14273 [22]. All joints were performed in a Harms & Wende RPS 100 welding machine using the shoulder plunge variant, with a rotation speed (*RS*) of 1300 rpm, a 2.6 mm plunge depth (*PD*) and plunge speed (*PS*) of 1.3 mm/s. Sufficient time between each weld was allowed to ensure repeatable conditions. The temperature at the clamping ring was kept below 40 °C.

2.3. Metallographic analysis

Weld's cross-section among the initial 1350 welds were analyzed in order to verify the influence of tool wear on particular joints features that could be associated to the trend of reduction of *LSS* observed in the experiment. In this regard, samples for macrographic examination were produced every

Table 1 – Chemical composition, surface heat tretament and mechanical properties of Hotvar®.

Chemical composition (% wt.) [21]	C	Si	Mn	Cr	Mo	V
	0.55	1.0	0.8	2.6	2.3	0.9
Surface hardening heat treatment	Plasma nitriding – 10 h at 480 °C					
Hardness	56 HRC					
Approximate yield strength [21]	1820 MPa					

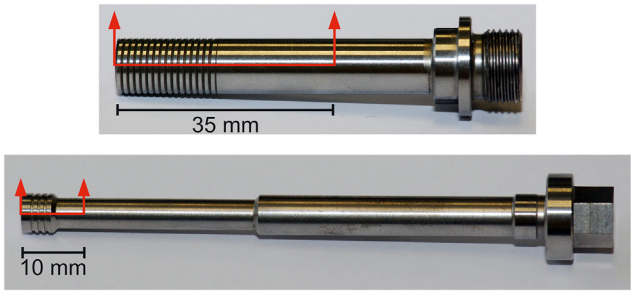

Fig. 3 – As-received shoulder and probe indicating the selected planes for profile measurement.

200 welds among the first 1350 welds. Specimens were embedded on transparent resin, ground and polished accordingly to metallographic specimen preparation procedures and etched by Keller's reagent (2 ml HF, 3 ml HCl, 5 ml HNO_3 and 190 ml water). Macrographs were acquired using a Leica IRM optical microscope with the attached Leica DFC 296 camera. The measurements of the stirred zone (SZ) area were performed with the ImageJ 1.51 k [23] image analysis software. The contrast between different welding regions was maximized in the macrographs (based on different grain sizes and shapes) to allow the identification of the *SZ area*. For this purpose, the macrographs were transformed into binary images, in which the isolated *SZ area* pixels are displayed as black, allowing the measurement of the *SZ area*.

2.4. *Mechanical testing*

To comprehend the effect of wear on joints' performance behavior along with the 2350 welding cycles, lap shear tests were carried out in regular intervals, measuring a sequence of three consecutive welds. In the initial 100 cycles, this interval was 20 welds and afterwards each 50 welds. These *LSS* tests were performed in accordance to ISO 14273 [22] in a Zwick-Roell 1478 testing machine at a constant displacement velocity of 1 mm/s.

3. Results and discussion

3.1. *Tool wear and wear mechanisms*

Changes in tool profiles allow the qualitative and quantitative evaluation of tool wear. Figure 4(a) shows the visual aspect of the tip of the probe at different stages of the analysis (s_0, s_{1350} and s_{2350}). The probe surface shows a slight decrease in brightness along the increasing number of welds performed, indicating changes in the surface roughness. Nonetheless, the tool geometry in all three cases is comparable in practical terms, i.e., no geometry changes can be associated to wear along the repeated welds. Profilometer-assessed

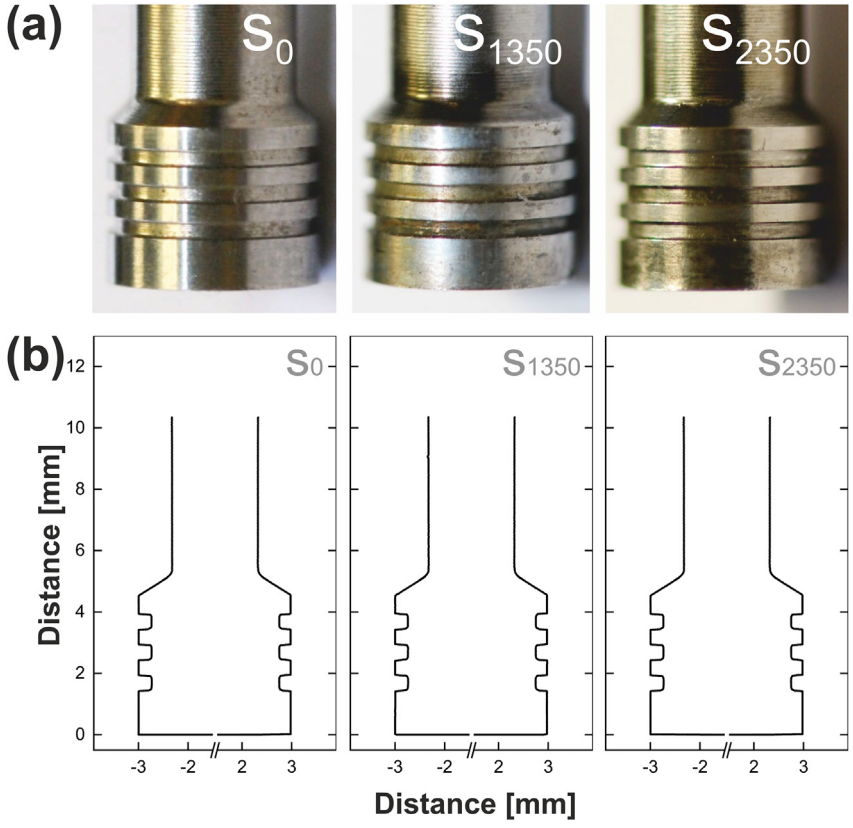

Fig. 4 – (a) Visual aspects and (b) profile measurements of the probe tip along increasing number of welds: as-received condition (s_0), after 1350 (s_{1350}) and 2350 (s_{2350}) weld spots.

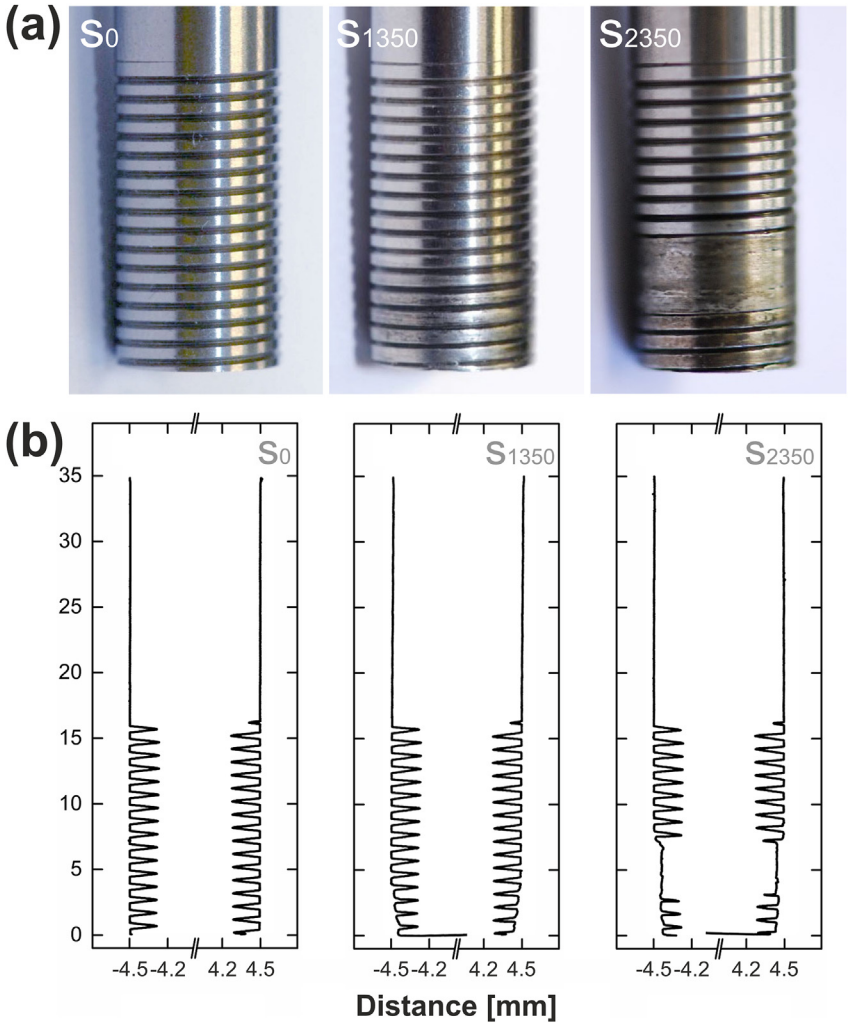

Fig. 5 – (a) Visual aspects and (b) profile measurements of the shoulder tip along increasing number of welds: as-received condition (s_0), after 1350 (s_{1350}) and 2350 (s_{2350}) weld spots.

measurements, shown in Fig. 4(b) were performed at the same stages of evaluation, proving that the profiles are nearly identical after the different number of performed welds, pointing out that the probe did not suffer noticeable wear. Since the shoulder plunge (Fig. 2) process variant is used, only the bottom of the probe is in frictional contact with the base material during the refilling phase, when the plasticized-displaced material is pushed back into its original place. Overall, the thermal-mechanical loading conditions are not severe enough to trigger the appearance of considerable wear effects on the probe.

In contrast, the inner and outer shoulder surfaces experience high shear stresses and temperature cycles during the process. The shoulder's visual analysis and profile measurements are presented in Fig. 5 (a) and (b), respectively. Unlike the probe, it is possible to observe progressive changes on the shoulder surface along with the number of spot welds. As a result of the first 1350 welds (s_{1350}), the reduction in surface brightness indicates an increase in surface roughness, considerably larger than observed on the probe. Furthermore, the comparison between s_0 to s_{1350} indicates changes on the shoulder threads profile for approximately 2.8 mm, starting from its tip. At the edge of the tool, where the most significant profile differences are noted, the reduction of tool external diameter is approximately 0.1 mm. With further welding cycles, the shoulder's visual analysis and measured profile at s_{2350} reveal changes along the adjacent region, extended to approximately 5 mm. Here, the shoulder threads are no longer noticeable.

The first prevailing wear mechanism identified at the tip of the shoulder is adhesive wear. The heat input and shearing undergone by the interface between shoulder and base material after the consecutive welds enable the formation of brittle Fe–Al and Fe–Li intermetallic layers at the tool surface, which fracture and detach from the tool during the welding process, resulting in adhesive wear. This hypothesis is supported by the findings from Lauterbach et al. [19], where evidence of Al diffusion on the Fe-based tool was found after 6400 refill friction stir spot welds of dissimilar AA5083-AA7020 and AA5083-AA6082 sheets. Similarly, the work of Nasiri et al. [10] also suggests the diffusion of Al and Li from the AA2099 sheet into a Hotvar® tool material. However, the latter study may

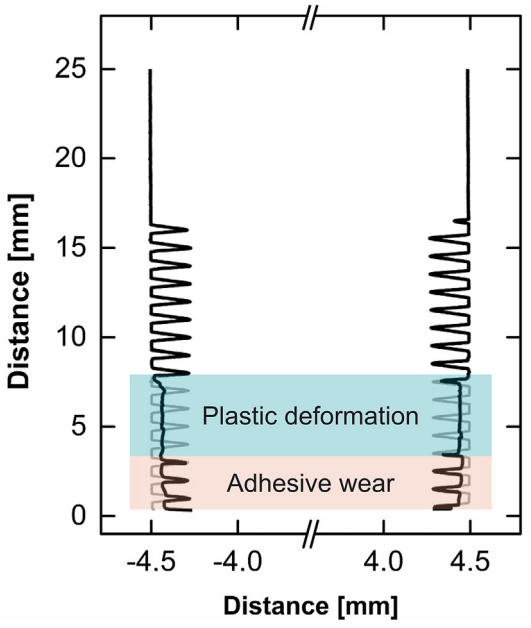

Fig. 6 – Wear mechanisms based on shoulder profile measurement of as-received tool (s_0 - grey line) and worn tool after 2350 weld spots (s_{2350} - black line).

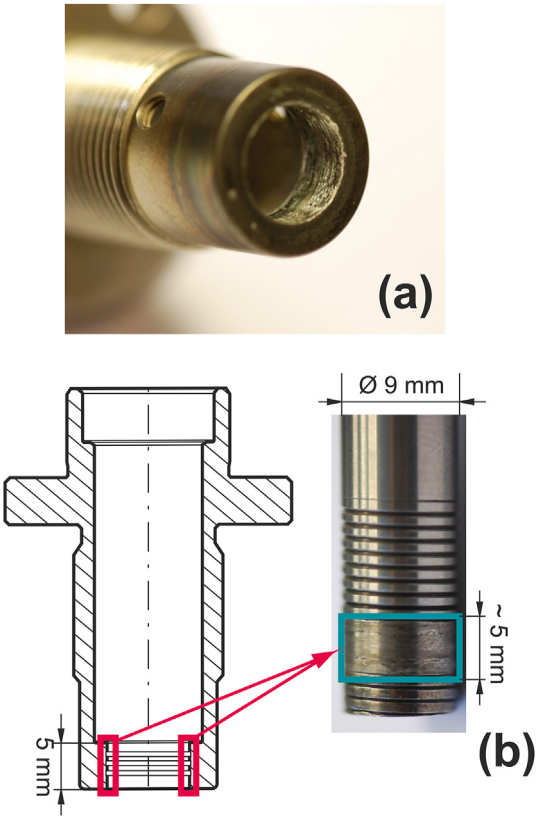

Fig. 7 – (a) Trapped aluminum inside the clamping ring inner surface. (b) Schematic representation of clamping ring indicating the region in frictional contact with shoulder (left) and the corresponding deformed region of the shoulder from 1350 weld spots onwards (right).

not be representative because of the tool's premature failure after only a few welds.

Fig. 6 shows the profile measurements of the shoulder for the as-received tool (s_0 - grey line) and the worn shoulder condition (s_{2350} - black line). Two distinct regions associated with the profile changes are observed, highlighted as adhesive wear zone (orange) and plastic deformation zone (blue). The plastic deformation zone appears around 2.8 mm from the shoulder's tip and remains for a length of approximately 5.0 mm. No direct contact between this region and the sheet material is expected, since it first appears on a point beyond the set *PD*. Although the adhesive wear may play a role in this zone as well, but the modifications on the shoulder's profile at s_{2350} points to a second wear mechanism. More than the average reduction of approximately 0.1 mm of the shoulder's external diameter, the disappearance of threads is an evidence of the effect of plastic deformation. It is concluded that the plastic deformation started at some point between welds 1350 and 2350, since no plastic deformation was observed on s_{1350}.

As mentioned above, this second type of wear is observed starting at the distance of around 2.8 mm from the shoulder's tip, which roughly matches the maximum plunge depth set (2.6 mm). A similar effect was reported by Montag et al. [18] using a plunge depth of 2.1 mm, considering that the most significant tool wear observed in the study was found at a distance of 2.0 mm from the shoulder's tip. According to their work, the effect results from the plunging and retracting of the shoulder during the process, which causes high stresses in this region due to the frictional contact with the lower area of the clamping ring. Besides, the authors explained that the more wear this particular area suffers, the more the workpiece material is pressed into the gaps between the tool parts, leading to progressively higher torques and temperatures during the welding process. This condition results in softening of tool material and an increase in the observed damage.

Fig. 7 shows the trapped workpiece material on the clamping ring inner surface after 1350 welds (a), and the matching length of the inner clamping ring surface and worn area of the shoulder (b). This observation supports the assumption that wear in this region most likely results from the interaction between these two tool elements. The effect of the progressive wear at the shoulder's tip observed until s_{1350} leads to an increasing gap between the inner surface of the clamping ring and the shoulder's worn exterior, which then traps the upwards-extruded workpiece material. As the volume of the gap between shoulder and clamping ring increases, oscillations of the shoulder around the tool rotational axis can produce increasingly higher amplitudes of the oscillatory motion at the tip of the tool, considering that the restriction caused by the clamping ring is progressively diminished. Thus, any instability of the rotating shoulder associated with its axial movement during the plunging and retracting stages can result in impacts of its surface against the fixed clamping ring, causing the observed plastic deformation wear mechanism. This effect could be magnified due to potential issues related to the assembly of the tool set, in cases when the tool rotating parts are not properly aligned to the tool rotational axis, resulting in higher amplitudes and, therefore, higher wear.

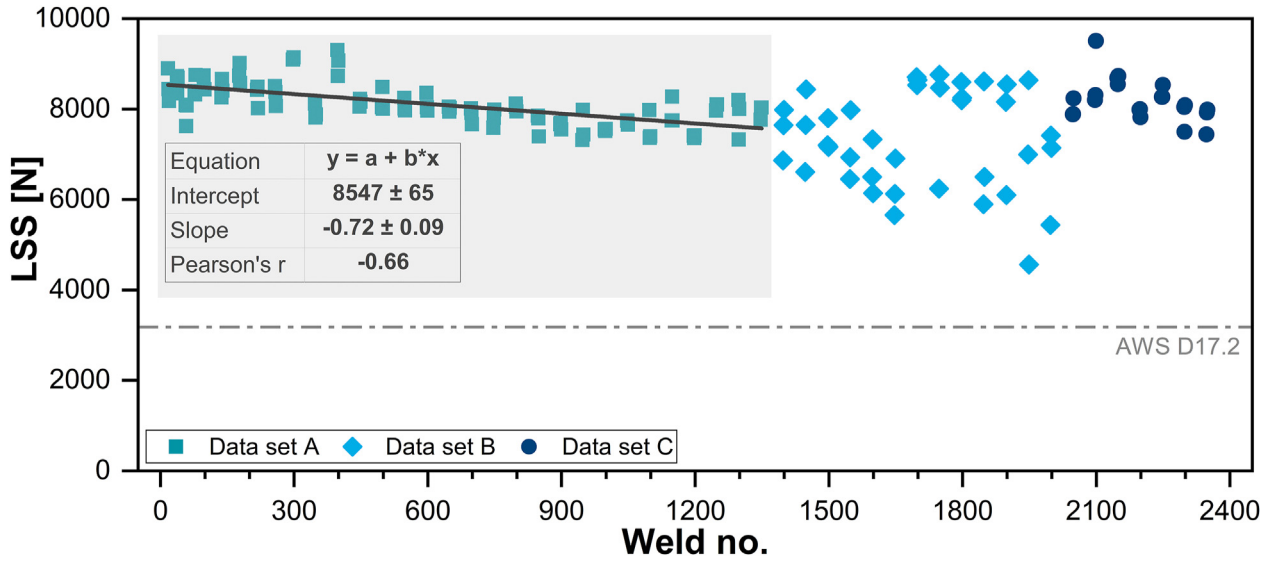

Fig. 8 – Lap shear strength (*LSS*) along 2350 weld spots split into three data sets (A, B and C), highlighting the linear regression of data set A's *LSS*. The dashed line indicates minimum requirements for resistance spot welds' *LSS* response according to AWS D17.2 [24].

3.2. *Effect of wear on joints mechanical properties*

The *LSS* values for the 155 investigated welds are shown in Fig. 8(a). *LSS* values vary roughly from 4500 to 9500 N, significantly exceeding the minimum of 3635 N required by spot welds of AA2198-T8 1.6 mm-thick sheets for aeronautic applications, according to AWS D17.2 [24].

The *LSS* data has to be divided into three data sets, delimited by each point of disassembly of the tool, cleaning, characterization and reassembly. Despite the variation observed throughout data set A and C, data set B shows a considerably larger variance in the *LSS*'s results. For the first data set A, defined until weld 1350, a clear tendency of strength reduction along with the welding cycles is observed. The Pearson's correlation coefficient ($r = -0.66$) indicates a moderate-to-large negative correlation between *LSS* and the welding cycles on this interval. This represents an average trend of reduction in welds' mechanical resistance by 720 N per 1000 cycles. This observation contradicts those reported by Montag et al. [18] that show no dependence of *LSS* and wear on the shoulder during the refill FSSW of AA6082-T6 2 mm-thick sheets. Data set C in itself shows a similar trend of decrease in LSS along the number of welding cycles. The *LSS* behavior observed in data set B differs from the one observed among the last 350 welds. This behavior of the second phase within this data set is unexpected and may be related to the presence of external sources of errors for the process, most probably related to the tool assembly considering the modifications on tool profile as discussed previously.

Although the welding tool did not fail during the production of the 2350 spot welds, the collected data is insufficient to predict the full tool life cycle, as more data on the failure of these components has to be collected in order to reach any conclusions about their life expectancy or their modes of failure. Besides, it is unclear whether the tool would ever begin producing welds that would not conform to AWS D17.2 before failing. As has been observed, there is evidence of non-reproductible behavior related to the *LSS* values between 1350 and 2000 welds. Because of the damage that has been caused by the likely unsuccessful assembly of the tool during these

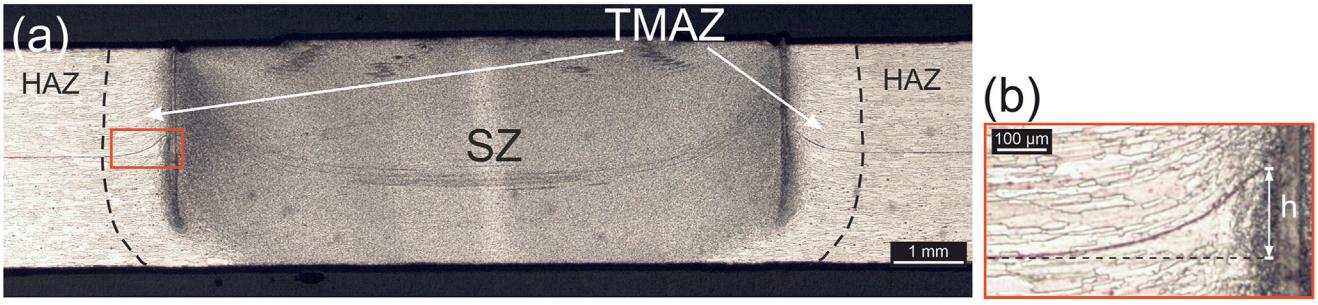

Fig. 9 – (a) Schematic representation of stirred zone (SZ) and thermo-mechanically affected zone (TMAZ) of one of the first weld cross-section obtained with the as-received tool and (b) hook feature in higher magnification (marked as a rectangle in (a)) indicating the hook height feature *h*.

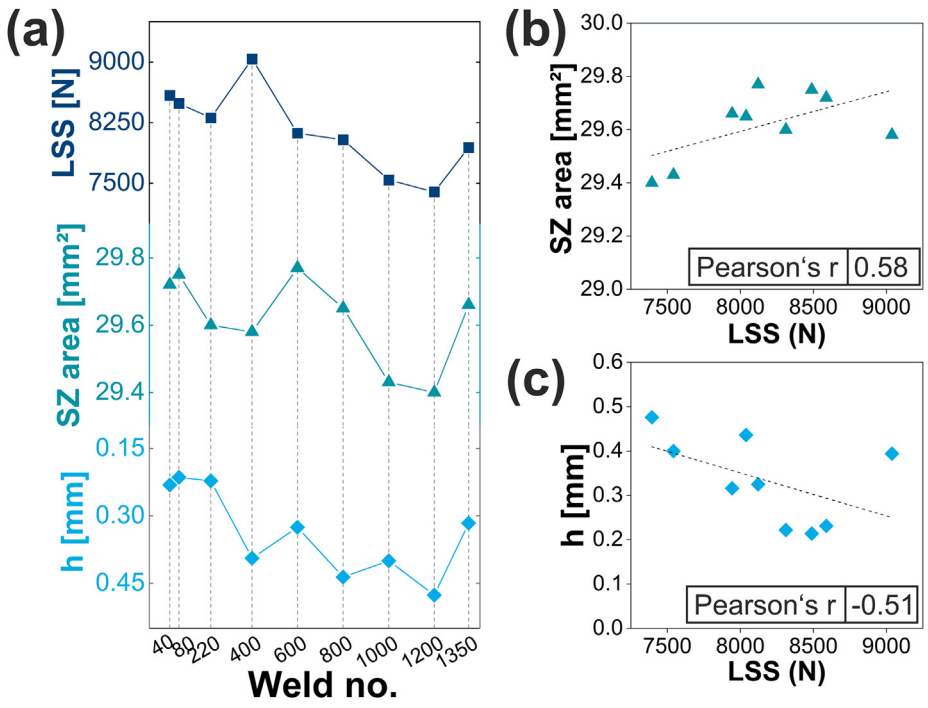

Fig. 10 – (a) Lap shear strength (*LSS*), stirred zone area (*SZ area*) and hook height (h – reversed axis) for selected welds and Pearson's correlation plots for (b) *SZ area* and (c) hook height *h* along with *LSS*.

welds (i.e. 1350 and 2000), some questions have been raised about whether going on (with an even higher count for the number of welds) would be representative of industrial environment and conditions. For this reason, the authors are convinced that future studies will be able to acquire relevant data on the actual life cycle of refill FSSW tools by basing their experimental strategies on studies such as the present one.

3.3. *The effect of wear on joints macroscopic features*

Fig. 9(a) shows a representative cross-section of the produced welds. The macrostructural features observed match the structure typically found in refill FSSW joints of aluminum alloy sheets [12]. Three distinct regions formed by the action of deformation and heat are identified: (i) heat-affected zone (HAZ), associated with transformations due to the increase of temperature during the process; (ii) thermo-mechanically affected zone (TMAZ), identified by long-and-bent-forwards grains around the weld nugget due to the deformation caused by the shoulder retraction combined with the generated heat; and (iii) SZ, the fine-equiaxed microstructure resulted from dynamic recrystallization of the intensively deformed material during the refill FSSW combined with the frictional-heat input. All analyzed macrographs were free of defects such as voids and lack of refill.

The effects of tool wear can be related to several aspects regarding the welding process, and consequently the joint macrostructure. Among these, two particular macrostructural features, *SZ area* and hook height *h*, were identified to correlate well with the *LSS* along the first 1350 welds, where a trend of reduction of *LSS* with the number of weld cycles was observed, as previously discussed. The hook, see Fig. 9(b), is a geometric feature found at the transitional-and-partially-bonded zone formed at the interface of the sheets and adjacent to the SZ. This feature is often evaluated in terms of its height *h* [25], i.e., the distance between the sheet interface level and the peak of the hook.

Fig. 10(a) presents the hook height *h* for selected samples along with their correspondent *LSS* mean values, with a coefficient of variation (CV) of 29.2%. By plotting the hook height reversely, Fig. 10(a), the trends of *LSS* and *h* match quite well, suggesting a negative correlation among these two properties. The Pearson's correlation coefficient presented in Fig. 10(b) ($r = -0.51$) indicates a moderate negative correlation between *h* and *LSS*. This inverse relationship was also found by Cao et al. [25] in AA6061 and Barros et al. [26] for AA2198 welds. In both cases, the reduction of *LSS* values along the hook height is explained as a result of the reduction of sheet effective thickness to resist the applied load.

Similarly to FSSW [27], the hook is formed due to the upward bending at the sheet interface caused by the plunge of the shoulder in the lower sheet. As discussed before, tool wear on the shoulder surface during the first phase of evaluation (Fig. 5) led to profile modifications (reduction of external diameter), especially at the tip of the tool, representing the part of the shoulder that plunged into the lower sheet and is responsible for its material flow and formation of the hook. Lage [28] investigated the formation of the hook in refill FSSW joints produced by aluminum alloys 5xxx sheets using the stop-action technique. The study points out that the tool geometry may be a key factor for the control of the hook formation since its mechanism is a consequence of the material

flow caused by both plunging and rotating movement of the shoulder. Investigations on the influence of FSSW tool geometry on the hook formation suggest that changes in the material flow due to these different geometries impact the hook morphology [29]. Thus, the reduction of approximately 0.1 mm shoulder's tip external diameter from s_0 to s_{1350} corresponds also to a reduction in terms of thread depth in this particular region of the shoulder, and thus, can progressively modify the material flow in thickness direction according to Badarinarayan et al. [29]. In conclusion, the tool wear observed in the shoulder causes modifications in the tool's profile, leading to changes in the material flow during the process, which can be associated with the trend of increasing the hook height.

The *SZ area* is another macrostructural feature identified to be related to the *LSS*. In a study on the refill FSSW of AA2198 sheets of two different thickness, De Castro et al. [30] identified that welds with a larger *SZ area* are associated with higher *LSS*. The *SZ area* of the selected cross-sections along their representative *LSS* is presented in Fig. 10(a). Except for a single point (after 400 welds), which exhibits a higher *LSS* value than expected for the correspondent *SZ area*, in comparison to the other joints, the plots suggest a positive correlation between *SZ area* and *LSS*. Pearson's coefficient ($r = 0.58$, Fig. 10(c)) confirms the moderate influence of *SZ area* on *LSS*. The trend of reduction for both *SZ area* and *LSS* throughout the welds production can be explained by the modification on the shoulder's profile. The progressive wear of the shoulder results in a reduction of the external diameter by 0.105 mm at its tip after the 1350 initial welding cycles, which means that material loss resulting from the wear mechanism represents a decrease of shoulder's volume. As consequence, this modification of the shoulder profile leads to a reduction of the plasticized sheet material displacement, resulting in a smaller recrystallized region. While the correspondence between the trends for *SZ area*, *LSS* and the inverse of the hook height could be verified, the CV for the *SZ area* is 0.44%, indicating that the *SZ area* variation is very limited.

4. Conclusions

The profile modifications of the probe and shoulder due to wear along 2350 welding cycles of AA2198-T8 sheets were analyzed, along with the investigation of the influence of these changes on mechanical and macrostructural features of the welds. The following conclusions are drawn based on experimental results.

- The probe did not suffer any considerable effect of wear, in contrast to the shoulder. The analysis of the shoulder's profile reveals adhesive wear at the tip. Plastic deformation was observed after 1350 welding cycles on the shoulder, around the matching area with the clamping ring, which most likely results from the interaction of these two tool elements.
- The joint average *LSS* has shown a decrease, by 720 N per 1000 cycles in the first 1350 cycles, illustrating a linear correlation between joint *LSS* and tool wear. Still, all produced 2350 welds exceeded the requirements of AWS D17.2 specification for aluminum resistance spot welds in aeronautic applications.
- The observation of cross-section features of selected joints among the initial 1350 produced welds indicates a trend in reduction in *SZ area* throughout the welding cycles, despite a low coefficient of variation. This progressive reduction in *SZ area* can be associated with the shoulder's profile changes, since it matches the decrease in external diameter that occurred at the shoulder's tip. Furthermore, a more significant effect (CV = 29.2%) of the modifications at the shoulder's profile is observed for the joints' hook height, which increase with the number of produced welds by the tool. This increase is likely due to changes in the material flow. Thus, the *LSS* behavior along the welding cycles matches the variation behavior of both *SZ area* and the inverse of the hook height.

Declaration of Competing Interest

The authors declare that they have no known competing financial interests or personal relationships that could have appeared to influence the work reported in this paper.

Acknowledgments

The authors gratefully acknowledge Wolfgang Limberg for the experimental work related to the profilometer measurements and Petra Fischer for the etching of the samples. This study was financed in part by the Coordenação de Aperfeiçoamento de Pessoal de Nível Superior – Brasil (CAPES) – Finance Code 001 and CNPq (National Council for Scientific and Technological Development – Brazil).

REFERENCES

[1] Sahlot P, Arora A. Numerical model for prediction of tool wear and worn-out pin profile during friction stir welding. Wear 2018;408–409:96–107. https://doi.org/10.1016/j.wear.2018.05.007.
[2] Miles MP, Ridges CS, Hovanski Y, Peterson J, Santella ML, Steel R. Impact of tool wear on joint strength in friction stir spot welding of DP 980 steel. Sci Technol Weld Join 2011;16:642–7. https://doi.org/10.1179/1362171811Y.0000000047.
[3] Bozkurt Y, Boumerzoug Z. Tool material effect on the friction stir butt welding of AA2124-T4 Alloy Matrix MMC. J Mater Res Technol 2018;7:29–38. https://doi.org/10.1016/j.jmrt.2017.04.001.
[4] Stolarski TA. Basic principles of tribology. Tribol Mach Des 1990:13–63. https://doi.org/10.1016/b978-0-08-051967-8.50005-0.
[5] Prado RA, Murr LE, Shindo DJ, Soto KF. Tool wear in the friction-stir welding of aluminum alloy 6061 + 20% Al2O3: a preliminary study. Scripta Mater 2001;45:75–80.
[6] Prado RA, Murr LE, Soto KF, McClure JC. Self-optimization in tool wear for friction-stir welding of Al 6061+20% Al2O3 MMC. Mater Sci Eng A 2003;349:156–65. https://doi.org/10.1016/S0921-5093(02)00750-5.
[7] Fernandez GJ, Murr LE. Characterization of tool wear and weld optimization in the friction-stir welding of cast

aluminum 359+20% SiC metal-matrix composite. Mater Char 2004;52:65–75. https://doi.org/10.1016/j.matchar.2004.03.004.
[8] Choi DH, Lee CY, Ahn BW, Choi JH, Yeon YM, Song K, et al. Frictional wear evaluation of WC–Co alloy tool in friction stir spot welding of low carbon steel plates. Int J Refract Met Hard Mater 2009;27:931–6. https://doi.org/10.1016/j.ijrmhm.2009.05.002.
[9] Wang J, Su J, Mishra RS, Xu R, Baumann JA. Tool wear mechanisms in friction stir welding of Ti–6Al–4V alloy. Wear 2014;321:25–32. https://doi.org/10.1016/j.wear.2014.09.010.
[10] Nasiri AM, Shen Z, Hou JSC, Gerlich AP. Failure analysis of tool used in refill friction stir spot welding of Al 2099 alloy. Eng Fail Anal 2018;84:25–33. https://doi.org/10.1016/j.engfailanal.2017.09.009.
[11] Schilling C, Dos Santos JF. Method and device for linking at least two adjoining work pieces by friction welding. European Patent Office; 2000EP1230062.
[12] Shen Z, Yang X, Yang S, Zhang Z, Yin Y. Microstructure and mechanical properties of friction spot welded 6061-T4 aluminum alloy. Mater Des 2014;54:766–78. https://doi.org/10.1016/j.matdes.2013.08.021.
[13] Fu B, Shen J, Suhuddin UFHR, Chen T, dos Santos JF, Klusemann B, et al. Improved mechanical properties of cast Mg alloy welds via texture weakening by differential rotation refill friction stir spot welding. Scripta Mater 2021;203:114113. https://doi.org/10.1016/j.scriptamat.2021.114113.
[14] Plaine AH, Gonzalez AR, Suhuddin UFH, dos Santos JF, Alcântara NG. The optimization of friction spot welding process parameters in AA6181-T4 and Ti6Al4V dissimilar joints. Mater Des 2015;83:36–41. https://doi.org/10.1016/j.matdes.2015.05.082.
[15] Geng P, Ma N, Ma H, Ma Y, Murakami K, Liu H, et al. Flat friction spot joining of aluminum alloy to carbon fiber reinforced polymer sheets: experiment and simulation. J Mater Sci Technol 2022;107:266–89.
[16] Iwashita T. Method and apparatus for joining. United States Patent; 2003US6601751B.
[17] Balasubramaniam GL, Boldsaikhan E, Fukada S, Fujimoto M, Kamimuki K. Effects of refill friction stir spot weld spacing and edge margin on mechanical properties of multi-spot-welded panels. J Manuf Mater Process 2020;4. https://doi.org/10.3390/JMMP4020055.
[18] Montag T, Wulfsberg J-P, Hameister H, Marschner R. Influence of tool wear on quality Criteria for refill friction stir spot welding (RFSSW) process. Procedia CIRP 2014;24:108–13. https://doi.org/10.1016/j.procir.2014.08.015.
[19] Lauterbach D, Keil D, Harms A, Leupold C, Dilger K. Tool wear behaviour and the influence of wear-resistant coatings during refill friction stir spot welding of aluminium alloys. Weld World 2021;65:243–50. https://doi.org/10.1007/s40194-020-01021-y.
[20] de Carvalho WS, Vioreanu MC, Lutz MRA, Cipriano GP, Amancio-Filho ST. The influence of tool wear on the mechanical performance of AA6061-T6 refill friction stir spot welds. Materials 2021;14. https://doi.org/10.3390/ma14237252.
[21] Uddeholm HOTVAR®. Technical data sheet 2011;Edition 4:1–12.
[22] International Organization for Standardization. ISO 14273:2016 - resistance welding - Destructive testing of welds - specimen dimensions and procedure for tensile shear testing resistance spot and embossed projection welds. 2016.
[23] Schneider CA, Rasband WS, Eliceiri KW. NIH Image to ImageJ: 25 years of image analysis. Nat Methods 2012;9:671–5. https://doi.org/10.1038/nmeth.2089.
[24] American Welding Society. Aws d17.2/d17.2m:2019 - specification for resistance welding for Aerospace applications 2019.
[25] Cao JY, Wang M, Kong L, Guo LJ. Hook formation and mechanical properties of friction spot welding in alloy 6061-T6. J Mater Process Technol 2016;230:254–62. https://doi.org/10.1016/j.jmatprotec.2015.11.026.
[26] Barros PAFDE, Campanelli LC, Alcântara NG, Santos JFDOS. An investigation on friction spot welding of AA2198-T8 thin sheets. 2016. https://doi.org/10.1111/ffe.12512.
[27] Badarinarayan H, Shi Y, Li X, Okamoto K. Effect of tool geometry on hook formation and static strength of friction stir spot welded aluminum 5754-O sheets. Int J Mach Tool Manufact 2009;49:814–23. https://doi.org/10.1016/j.ijmachtools.2009.06.001.
[28] Lage SBM. Otimização dos parâmetros de soldagem a ponto por Fricção (FSpW) da liga AlMgSc e avaliação das propriedades mecânicas estáticas e dinâmicas. Universidade Federal de Sao Carlos; 2017.
[29] Badarinarayan H, Yang Q, Zhu S. Effect of tool geometry on static strength of friction stir spot-welded aluminum alloy. Int J Mach Tool Manufact 2009;49:142–8. https://doi.org/10.1016/j.ijmachtools.2008.09.004.
[30] de Castro CC, Plaine AH, Dias GP, de Alcântara NG, dos Santos JF. Investigation of geometrical features on mechanical properties of AA2198 refill friction stir spot welds. J Manuf Process 2018;36:330–9. https://doi.org/10.1016/j.jmapro.2018.10.027.